Circular Rydberg states in parallel electric and magnetic fields

Hiroya Suno,[1] Lidija Andric,[1] Tasko P. Grozdanov,[1,2] and Ronald McCarroll[1]
[1]*Laboratoire de Dynamique des Ions, Atomes et Molécules (ESA 7066 du CNRS), Université Pierre et Marie Curie, 4 place Jussieu T12-B75, 75252 Paris Cedex 05, France*
[2]*Institute of Physics, P.O. Box 57, 11001 Belgrade, Yugoslavia*
(Received 17 June 1998)

Circular and nearby Rydberg states in parallel electric and magnetic fields are studied using semiclassical and exact quantum-mechanical methods. A wide range of external field strengths is considered including regimes close to and beyond the classical ionization thresholds. When the tunneling decay rates due to the presence of the electric field are negligible, semiclassical eigenvalues and wave functions represent very good approximations. The combination of the complex-coordinate method with a discrete variable representation and the Lanczos iterative scheme provides an efficient way to calculate exactly the complex eigenvalues corresponding to the resonances emerging from the quasibound circular and nearby Rydberg states. Magnetic fields have in general a stabilizing effect, diminishing the decay rates, although there are cases showing the nonmonotonic (oscillatory) dependences of the imaginary parts of the eigenvalues with increasing magnetic field strength. [S1050-2947(98)06012-0]

PACS number(s): 32.60.+i

I. INTRODUCTION

Atoms in circular Rydberg states are characterized by the maximum possible angular momentum ($l=|m|=n-1\gg 1$, where n,l,m are spherical quantum numbers) of the highly excited electron. The electron is localized in the vicinity of the Bohr circular orbit of the radius n^2 atomic units, which clearly indicates the semiclassical nature of these states. As the electron probability distribution does not penetrate the atomic core, atoms can be considered to be quasihydrogenic. These states are also characterized by very long radiative lifetimes, since the only allowed dipole transition is ($n\rightarrow n-1$; $|m|\rightarrow|m|-1$). They can also serve as approximations for two-level systems in studies of the electrodynamics of atoms in cavities [1]. Collision processes involving atoms in circular Rydberg states are characterized by a highly anisotropic cross section [2–4]. The first experimental realization of circular Rydberg states was accomplished in 1983 by Hulet and Kleppner [5], and since then various preparation schemes have been proposed and developed [6–12].

Studies of the behavior of circular Rydberg states under the influence of the external static fields is important, first because many of the preparation methods mentioned above involve application of these fields, and second because these systems are ideal for testing various semiclassical theories. In the present paper we shall be interested in comparing semiclassical and fully quantum descriptions of circular and nearby Rydberg states in relatively strong parallel electric and magnetic fields, that is, beyond the weak-field perturbational regime. This work is along the lines of previous investigations [13–15] which dealt with the case of pure magnetic fields. Here we shall investigate in particular new effects brought about by the presence of a strong electric field, such as the possibility of field ionization of an atom in a circular Rydberg state.

The plan of this paper is as follows. In Sec. II we present a semiclassical description of our system. Section III describes the quantum-mechanical method used to obtain exact results. Our results are presented in Sec. IV in the form of a comparison between the semiclassical and quantum-mechanical calculations. Finally, Sec. V contains concluding remarks.

II. SEMICLASSICAL METHOD

In our development of the semiclassical description of circular Rydberg states in parallel electric and magnetic fields, we follow the approach of Germann [14] previously used for the case of a pure magnetic field. This approach itself is a generalization of the method proposed by Bender *et al.* [16]. In addition, it is not difficult to see that it can be related to the semiclassical quantization of the phase-space tori located in the stability islands surrounding stable periodic orbits [17].

Representing the electron wave function in the form

$$\psi(\rho,z,\varphi)=(2\pi\rho)^{-1/2}\phi(\rho,z)\exp(im\varphi), \tag{2.1}$$

the Schrödinger equation in cylindrical coordinates and atomic units reads

$$\left[-\frac{1}{2}\left(\frac{\partial^2}{\partial\rho^2}+\frac{\partial^2}{\partial z^2}\right)+\frac{m^2-\frac{1}{4}}{2\rho^2}-\frac{1}{(\rho^2+z^2)^{1/2}}+\tfrac{1}{2}mB+\tfrac{1}{8}B^2\rho^2+Fz\right]\phi(\rho,z)=E\phi(\rho,z), \tag{2.2}$$

where m is the magnetic quantum number and B and F are the magnetic and electric fields strengths expressed in units of $B_0\approx 2.35\times 10^5 T$ and $F_0\approx 5.14\times 10^9$ V/cm.

Our goal is to look for the solutions of Eq. (2.2) in the limit $|m|\to\infty$. To this end, we choose as the small expansion parameter $\delta=(|m|+1)^{-1}\to 0$. This particular choice is discussed in Ref. [14] and it basically ensures the exact zero-field limit for the energy of the circular state [16]. Introducing the scaled quantities $\tilde{\rho}=\delta^2\rho$, $\tilde{z}=\delta^2 z$, $\tilde{B}=\delta^{-3}B$, $\tilde{F}=\delta^{-4}F$, and $\tilde{E}=\delta^{-2}(E-\frac{1}{2}mB)$, Eq. (2.2) is transformed to

$$\left[-\frac{\delta^2}{2}\left(\frac{\partial^2}{\partial\tilde{\rho}^2}+\frac{\partial^2}{\partial\tilde{z}^2}\right)+\frac{1-2\delta+\frac{3}{4}\delta^2}{2\tilde{\rho}^2}-\frac{1}{(\tilde{\rho}^2+\tilde{z}^2)^{1/2}}+\tfrac{1}{8}\tilde{B}^2\tilde{\rho}^2+\tilde{F}\tilde{z}\right]\phi(\tilde{\rho},\tilde{z})=\tilde{E}\,\phi(\tilde{\rho},\tilde{z}). \tag{2.3}$$

For $\delta\to 0$, the electron is localized at the minimum $(\tilde{\rho}_c,\tilde{z}_c)$ of the potential

$$V(\tilde{\rho},\tilde{z})=\frac{1}{2\tilde{\rho}^2}-\frac{1}{(\tilde{\rho}^2+\tilde{z}^2)^{1/2}}+\tfrac{1}{8}\tilde{B}^2\tilde{\rho}^2+\tilde{F}\tilde{z}. \tag{2.4}$$

Actually, in three dimensions the electron is localized around the circular orbit of radius $\tilde{\rho}=\tilde{\rho}_c$ located in the plane $\tilde{z}=\tilde{z}_c$. The position of the minimum is determined by the equations

$$\frac{\partial V}{\partial\tilde{z}}=\frac{\tilde{z}}{(\tilde{\rho}^2+\tilde{z}^2)^{3/2}}+\tilde{F}=0, \tag{2.5}$$

$$\frac{\partial V}{\partial\tilde{\rho}}=-\frac{1}{\tilde{\rho}^3}+\frac{\tilde{\rho}}{(\tilde{\rho}^2+\tilde{z}^2)^{3/2}}+\tfrac{1}{4}\tilde{B}^2\tilde{\rho}=0. \tag{2.6}$$

Introducing new δ-scaled displacement coordinates,

$$x_1=(\tilde{\rho}-\tilde{\rho}_c)\,\delta^{-1/2},\quad x_2=(\tilde{z}-\tilde{z}_c)\,\delta^{-1/2}, \tag{2.7}$$

and retaining in Eq. (2.3) terms up to the order of δ, we obtain

$$[V(\tilde{\rho}_c,\tilde{z}_c)+\delta H_0]\phi(x_1,x_2)=\tilde{E}\,\phi(x_1,x_2), \tag{2.8}$$

where

$$H_0=-\frac{1}{2}\left(\frac{\partial^2}{\partial x_1^2}+\frac{\partial^2}{\partial x_2^2}\right)+\tfrac{1}{2}\mathcal{A}x_1^2+\mathcal{B}x_1x_2+\tfrac{1}{2}\mathcal{C}x_2^2-\frac{1}{\tilde{\rho}_c^2}, \tag{2.9}$$

with

$$\mathcal{A}\equiv\left.\frac{\partial^2 V}{\partial\tilde{\rho}^2}\right|_{(\tilde{\rho},\tilde{z})=(\tilde{\rho}_c,\tilde{z}_c)}=\frac{3}{\tilde{\rho}_c^4}+\frac{\tilde{z}_c^2-2\tilde{\rho}_c^2}{(\tilde{\rho}_c^2+\tilde{z}_c^2)^{5/2}}+\tfrac{1}{4}\tilde{B}^2. \tag{2.10}$$

$$\mathcal{B}\equiv\left.\frac{\partial^2 V}{\partial\tilde{\rho}\,\partial\tilde{z}}\right|_{(\tilde{\rho},\tilde{z})=(\tilde{\rho}_c,\tilde{z}_c)}=-\frac{3\tilde{z}_c\tilde{\rho}_c}{(\tilde{\rho}_c^2+\tilde{z}_c^2)^{5/2}}, \tag{2.11}$$

$$\mathcal{C}\equiv\left.\frac{\partial^2 V}{\partial\tilde{z}^2}\right|_{(\tilde{\rho},\tilde{z})=(\tilde{\rho}_c,\tilde{z}_c)}=\frac{\tilde{\rho}_c^2-2\tilde{z}_c^2}{(\tilde{\rho}_c^2+\tilde{z}_c^2)^{5/2}}. \tag{2.12}$$

Changing to rotated coordinates (''normal modes''),

$$u=x_1\cos\theta+x_2\sin\theta, \tag{2.13}$$

$$v=-x_1\sin\theta+x_2\cos\theta, \tag{2.14}$$

where $\tan 2\theta=2\mathcal{B}/(\mathcal{A}-\mathcal{C})$, the Hamiltonian (2.9) is transformed into

$$H_0=-\frac{1}{2}\left(\frac{\partial^2}{\partial u^2}+\frac{\partial^2}{\partial v^2}\right)+\tfrac{1}{2}\omega_1^2u^2+\tfrac{1}{2}\omega_2^2v^2-\frac{1}{\tilde{\rho}_c^2}, \tag{2.15}$$

with

$$\omega_{1,2}^2=\tfrac{1}{2}\{\mathcal{A}+\mathcal{C}\pm[(\mathcal{A}-\mathcal{C})^2+4\mathcal{B}^2]^{1/2}\}. \tag{2.16}$$

The spectrum of H_0 is that of the two-dimensional harmonic oscillator, so that from Eq. (2.8) we finally find

$$E\approx\tfrac{1}{2}mB+\delta^2V(\tilde{\rho}_c,\tilde{z}_c)+\delta^3((\nu_1+\tfrac{1}{2})\omega_1+(\nu_2+\tfrac{1}{2})\omega_2-\tilde{\rho}_c^{-2}),\quad \nu_{1,2}=0,1,\ldots. \tag{2.17}$$

The circular states correspond to $\nu_1=\nu_2=0$ and we expect the above formula to be the most accurate in this case.

The approximate eigenfunctions $\phi_{m\nu_1\nu_2}(\rho,z)$ can be expressed in terms of those of the two-dimensional harmonic oscillator. For example, the circular states are described by the simple product of Gaussians:

$$\phi_{m00}(\rho,z)=\left(\frac{\omega_1\omega_2\delta^6}{\pi^2}\right)^{1/4}\exp(-\tfrac{1}{2}\omega_1u^2-\tfrac{1}{2}\omega_2v^2), \tag{2.18}$$

where u and v are related to ρ and z via relations (2.13), (2.14), and (2.7).

All the above considerations are meaningful under the condition that the minimum of the potential (that is, the circular orbit), determined by relations (2.5) and (2.6), exists. We can determine the range of the electric and magnetic field strengths for which such an orbit exists. To this end, let us introduce a new variable x through the relation $\tilde{z}=-\tilde{F}x^3$. Relations (2.5) and (2.6) than take the form

$$\tilde{\rho}^2=-\tilde{F}^2x^6+x^2, \tag{2.19}$$

$$x(1+\tfrac{1}{4}\tilde{B}^2x^3)(1-\tilde{F}^2x^4)^2=1. \tag{2.20}$$

It is clear that in order to determine $\tilde{z}_c$ and $\tilde{\rho}_c$ we have to solve only Eq. (2.20) in the domain $0<x<(\tilde{F})^{-1/2}$. The function on the left-hand side of this equation has a simple zero at $x=0$ and a double zero (that is a minimum) at $x=(\tilde{F})^{-1/2}$. In between there is a maximum whose coordinate x is determined by the equation

$$1-9\tilde{F}^2+\tilde{B}^2x^3(1-3\tilde{F}^2x^4)=0. \tag{2.21}$$

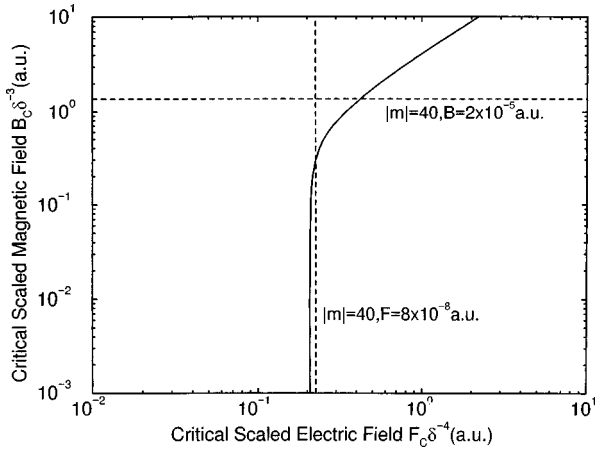

FIG. 1. Full line represents the critical curve defining the classical ionization threshold for circular states. Circular trajectories exist in the region left of the critical curve. Vertical and horizontal dashed lines are related to Figs. 4–7 and are discussed later in the text.

Now, if the maximum value of the left-hand side of Eq. (2.20) is larger than 1, then there are two roots in the interval $0<x<(\tilde{F})^{-1/2}$. The smaller one corresponds to a minimum of the effective potential (that is, to a stable circular orbit) while the larger one corresponds to a saddle point of the potential (that is, to an unstable circular orbit). The critical case occurs when both roots (orbits) merge. This situation corresponds to a *classical ionization threshold of the circular state* and is realized if both relations (2.20) and (2.21) are simultaneously fulfilled. The elimination of x from these two equations leads to a functional dependence between $\tilde{F}$ and $\tilde{B}$ defining a critical curve in the $(\tilde{F},\tilde{B})$ plane representing the border of the existence of the circular orbits. This curve can easily be determined numerically and is shown in Fig. 1. The region on the left of the curve corresponds to the values of $\tilde{F}$ and $\tilde{B}$ for which the circular orbits exist. The stabilizing effect of the magnetic field can be seen from Fig. 1: the stronger the magnetic field, the stronger the electric field needed to reach the classical ionization threshold.

In the limit of very small magnetic fields $\tilde{B}\ll 1$, it is not difficult to obtain an analytical relation defining the critical curve:

$$\tilde{B}_c=\tfrac{27}{4}\tilde{F}_c^{3/4}\left[\tilde{F}_c^{1/2}-\frac{2^6}{3^{9/2}}\right]^{1/2}. \tag{2.22}$$

This expression gives for the classical ionization threshold of circular states in pure electric fields the value $\tilde{F}_c=2^{12}/3^9$, which is in accord with earlier findings of Bender *et al.* [16]. When both fields are large, $\tilde{B}\gg 1$ and $\tilde{F}\gg 1$, the critical curve asymptotically approaches the following one:

$$\tilde{B}_c=\tilde{F}_c\left(27-\frac{12}{(\tilde{F}_c^2)^{1/4}}\right)^{1/2}. \tag{2.23}$$

III. EXACT QUANTUM CALCULATIONS

Strictly speaking, the spectrum of the Hamiltonian describing a hydrogen atom in parallel electric and magnetic fields is continuous. However, as is well known, for relatively weak electric fields one can define quasibound states or resonances with exponentially small decay rates corresponding to tunneling transitions leading to field ionization of the atom. The decay rates increase with the increase of the electric field strength and, once the classical ionization threshold is approached, are no longer exponentially small. The circular Rydberg states in this respect are no exceptions, and our intention here is to study the corresponding resonances in various regimes of the external fields strengths.

In general, the resonances are associated with the complex poles of the system's Green's function or S matrix [18], located on nonphysical sheets of the Riemann surface of complex energies. The real part of a complex pole E_n is usually called the resonance position ($E_r=\mathrm{Re}\,E_n$) while the width (or decay rate) is related to the imaginary part ($\Gamma=-2\,\mathrm{Im}\,E_n$).

The method widely used to determine resonances is the complex coordinate (or rotation, or scaling, or dilatation) method (for a review, see [19,20]). When applied to a hydrogen atom in external fields, it consists in replacing the electron coordinate and momentum operators by complex quantities:

$$\vec{r}\rightarrow\vec{r}e^{i\theta},\quad \vec{p}\rightarrow\vec{p}e^{-i\theta}, \tag{3.1}$$

where θ is a real ''rotation angle.'' The transformed Hamiltonian $H(\theta)$ is a non-Hermitian operator and has a complex spectrum which can be related to the spectrum and resonances corresponding to the original Hamiltonian $H=H(\theta=0)$. In general, the bound (real discrete) spectrum is common to both H and $H(\theta)$, as well as the positions of all continuum thresholds. The continua themselves, however, are rotated by the angle -2θ into the lower half of the complex energy plane. The resonances of H are the discrete complex eigenvalues of $H(\theta)$ and are independent of θ provided they are uncovered by the rotation. The case of the Stark effect is special, because then the continuum spectrum extends from $-\infty$ to $+\infty$ and there is no threshold. Herbst [21] has shown that in that case the continuous spectrum disappears completely and only discrete resonances remain.

In our problem, after performing the transformation (3.1) and introducing the scaled parabolic coordinates

$$\frac{u}{\lambda}=(\rho^2+z^2)^{1/2}+z, \tag{3.2}$$

$$\frac{v}{\lambda}=(\rho^2+z^2)^{1/2}-z, \tag{3.3}$$

$$\rho d\rho dz=\frac{1}{4\lambda^3}(u+v)dudv, \tag{3.4}$$

with an arbitrary scaling parameter λ, the complex-rotated Hamiltonian, restricted to a subspace with fixed magnetic quantum number m, takes the form

$$H(\theta)=e^{-i2\theta}T-e^{-i\theta}\frac{2\lambda}{u+v}+e^{i2\theta}\frac{B^2}{8\lambda^2}uv$$

$$+e^{i\theta}\frac{u-v}{2\lambda}F+\tfrac{1}{2}mB, \tag{3.5}$$

with the kinetic energy operator given by

$$T=\frac{2\lambda^2}{u+v}\left[-\frac{\partial}{\partial u}u\frac{\partial}{\partial u}-\frac{\partial}{\partial v}v\frac{\partial}{\partial v}+\frac{m^2}{4}\left(\frac{1}{u}+\frac{1}{v}\right)\right]. \tag{3.6}$$

Next we construct the Hamiltonian matrix corresponding to Eq. (3.5) by using a discrete variable representation (DVR) [22]. The particular basis used is the direct product of two one-dimensional DVR's corresponding to coordinates u and v and related to generalized Gauss-Laguerre quadrature points and weights [15]. This DVR is equivalent to a ''Laguerre mesh'' introduced previously by Baye and Vincke [23]. Details about the basis functions and matrix element can be found in our recent work [15], where it was applied to the case of a pure magnetic field. The only difference in the present case is that the parity $\Pi(z\rightarrow -z)$ is no longer a good quantum number, and therefore the DVR basis could not be symmetrized. It is important to emphasize that the matrix representing the potential energy is diagonal while the matrix representing the kinetic energy is sparse [15]. Therefore, DVR is well suited for the applications of various iterative methods relying on the repetitions of the basic matrix-vector multiplication operation.

In order to extract the resonance eigenvalues of the circular and nearby states, we have adopted the complex Lanczos recursion method (see, for example, [24]). As a good starting vector for the Lanczos recursions, one can use the semiclassical wave function of the type (2.18). In a series of calculations for various field strengths, one can always use as an initial Lanczos vector the eigenvector previously found for the nearby field strengths. For the typical results presented in the next section, related to the $|m|=40$ manifolds and laboratory-strength fields, a few hundred iterations were sufficient to obtain converged results with an accuracy of eight significant figures, while using DVR bases sets of dimensions in the range from $35\times 35=1225$ to $45\times 45=2025$. Careful checks are performed to prove that the results are stationary with respect to variations of the scaling parameter λ and rotation angle θ.

IV. RESULTS AND DISCUSSION

We first analyze the pure Stark effect for the circular and nearby Rydberg states. Figure 2 shows the field dependence of the resonance positions (real parts of complex eigenvalues) for the circular states with $|m|=40$ and for the first two excited states in the same manifold. States are labeled by the semiclassical quantum numbers ν_1 and ν_2 from Eq. (2.17), which in the zero-field limit correspond to usual hydrogenic parabolic quantum numbers. Semiclassical eigenvalues are shown as dashed lines. In this figure (as well as in all others), the quantum and semiclassical results for the circular Rydberg states $(\nu_1,\nu_2)=(0,0)$ are almost visually indistinguishable, up to the fields close to the classical ionization threshold (shown as a vertical line in Fig. 2). The agreement between the semiclassical and quantum results for higher states in the manifold is not so good, but still satisfactory, as can be seen from Fig. 2.

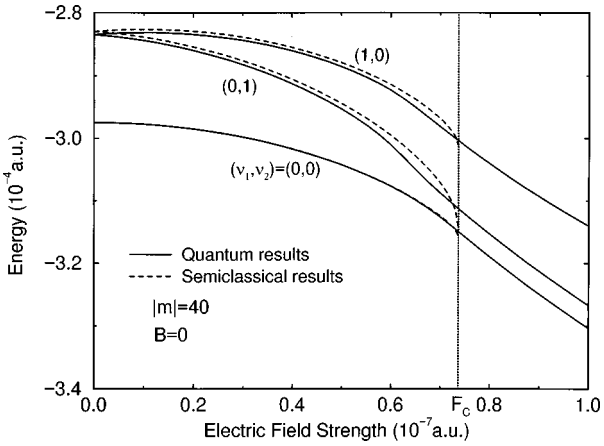

FIG. 2. Full lines represent the real parts of the complex resonance eigenvalues ($|m|=40$) for circular and nearby states in zero magnetic and varying electric field. Dashed lines are semiclassical approximations and quantum numbers (ν_1,ν_2) are defined in Eq. (2.17). Vertical line at $F_c=7.36\times 10^{-8}$ corresponds to classical ionization threshold of the circular state.

Figure 3 shows the electric-field dependence of widths (two times the negative imaginary part of the complex eigenvalues) for the same three states considered in Fig. 2. Here, we can see the exponential increase of the widths up to the classical ionization threshold and the subsequent slower increase with the field strength.

Next we consider the change of resonance parameters of circular $(m=-40)$ and nearby Rydberg states for fixed electric field $F=8\times 10^{-8}$ and increasing the magnetic field from $B=0$ to $B=1.2\times 10^{-5}$. This corresponds to moving along the vertical line intersecting the critical curve in Fig. 1.

Figure 4 shows the dependence of the real parts of the eigenvalues on magnetic field strength. We observe a monotonic decrease which is well approximated with the semiclassical results in the region of the existence of the circular orbits.

The stabilizing effect of the magnetic field can be seen in

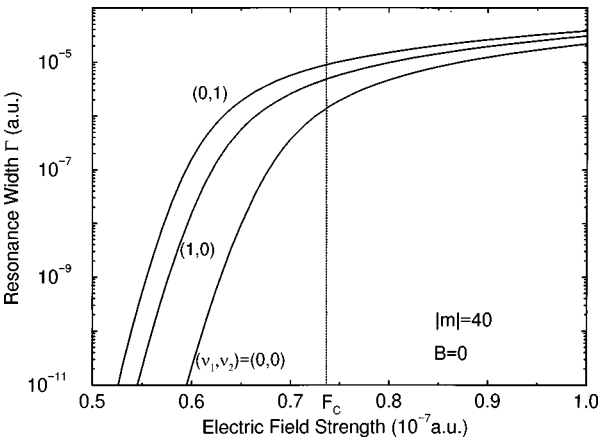

FIG. 3. Resonance widths of the states whose real parts of the eigenvalues are shown in Fig. 2.

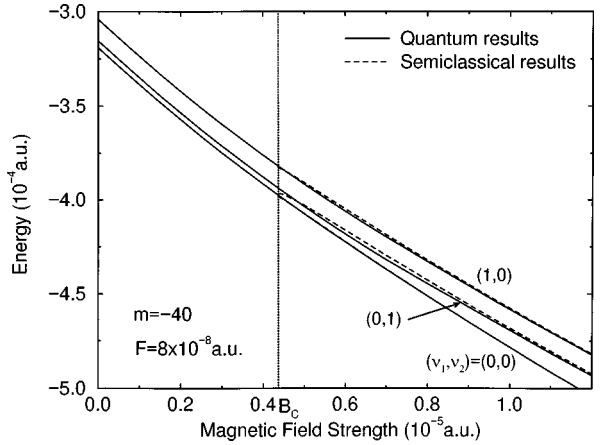

FIG. 4. Full lines represent the real parts of the complex resonance eigenvalues ($m=-40$) for circular and nearby states for fixed electric field strength of $F=8\times10^{-8}$ and varying magnetic field. Dashed lines are semiclassical approximations and quantum numbers (ν_1,ν_2) are defined in Eq. (2.17). Vertical line at $B_c=4.37\times10^{-6}$ corresponds to classical ionization threshold of the circular state.

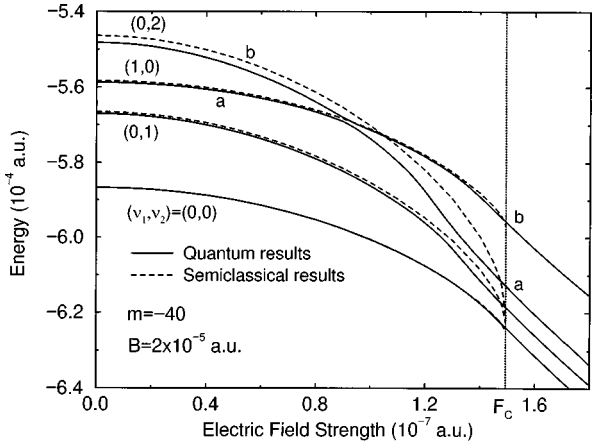

FIG. 6. Full lines represent the real parts of the complex resonance eigenvalues ($m=-40$) for circular and nearby states for fixed magnetic field strength of $B=2\times10^{-5}$ and varying electric field. Dashed lines are semiclassical approximations and quantum numbers (ν_1,ν_2) are defined in Eq. (2.17). Vertical line at $F_c=1.49\times10^{-7}$ corresponds to classical ionization threshold of the circular state.

Fig. 5, which shows the decrease of the widths with the increasing magnetic field strength. Note, however, that the decrease may not be monotonic, as is the case with the state $(\nu_1,\nu_2)=(1,0)$ in Fig. 5. This phenomenon of oscillatory behavior of the imaginary parts of the resonances with increasing magnetic field strength has also been noticed in a study of resonances belonging to the $m=0$ manifold of the hydrogen atom in parallel electric and magnetic fields [25].

The last case considered is the one in which the magnetic field strength is fixed at $B=2\times10^{-5}$ and the electric field strength increases from $F=0$ to $F=1.8\times10^{-7}$. This corresponds to moving along the horizontal line, shown in Fig. 1, that is, observing the transition from a stable to an unstable (with respect to field ionization) regime.

Figure 6 shows the behavior of the real parts of the eigenvalues as functions of the electric field strength. One can see that the state labeled by the semiclassical quantum numbers $(\nu_1,\nu_2)=(1,0)$ at small electric field strengths undergoes an avoiding crossing with the state labeled (0,2) at small fields. Obviously, for this last state the semiclassical approximation is the least accurate, so that the crossing point of the semiclassical approximants is considerably displaced from the avoided crossing region. In order to avoid confusion we have attached in Fig. 6 labels *a-a* and *b-b* to exact quantum adiabatic states.

Figure 7 shows the evolutions of the corresponding widths with the increase of the electric field strength. Just like in all preceding cases, the dependence is strictly monotonic for the circular state (0,0). However, in the case of the *b-b* state, as seen from Fig. 7, an oscillation similar to that in Fig. 5 is observed. This fact, together with the results of the previously mention work [25], suggests that this oscillatory behavior is a generic property of the Rydberg-state resonances in external fields.

In order to provide more quantitative information, we present the numerical values of the calculated quantum and semiclassical energies. Table I gives a series of results for the $|m|=40$ manifolds and for combinations of field strengths when the widths are completely negligible. The inspection of Table I confirms that the semiclassical esti-

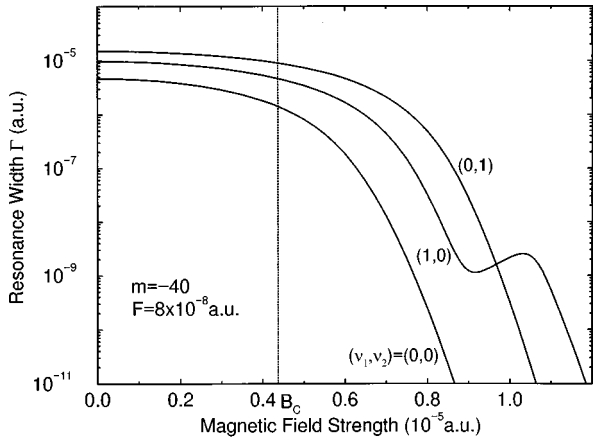

FIG. 5. Resonance widths of the states whose real parts of the eigenvalues are shown in Fig. 4.

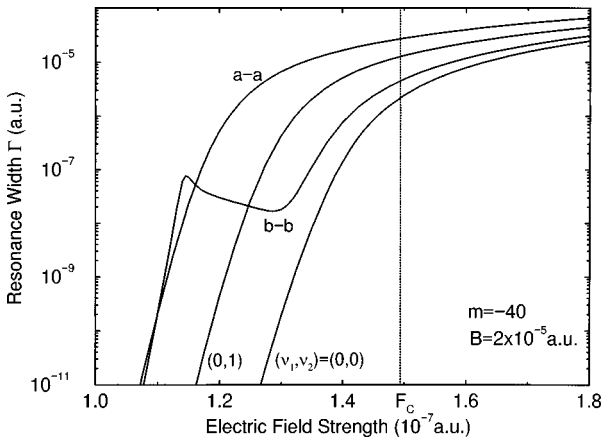

FIG. 7. Resonance widths of the states whose real parts of the eigenvalues are shown in Fig. 6.

TABLE I. Comparison of the calculated quantum eigenenergies E (in a.u.) of circular and near-circular states corresponding to $m=-40$ with semiclassical estimates E^{SC} for various fields (in a.u.) in the region where the widths are negligible. The energies of the states with $m=+40$ are obtained by adding mB. Numbers in square brackets indicate powers of ten.

		$F=0$		$F=0.5[-7]$	
B	(ν_1,ν_2)	E	E^{SC}	E	E^{SC}
0	(0,0)	−2.974 420 0[−4]	−2.974 420 0[−4]	−3.042 130 8[−4]	−3.042 027 0[−4]
	(0,1)	−2.834 467 1[−4]	−2.829 326 3[−4]	−2.952 302 5[−4]	−2.943 701 3[−4]
	(1,0)	−2.834 467 1[−4]	−2.829 326 3[−4]	−2.885 016 8[−4]	−2.878 755 8[−4]
0.5[−5]	(0,0)	−3.886 558 2[−4]	−3.886 554 3[−4]	−3.947 806 0[−4]	−3.947 740 6[−4]
	(0,1)	−3.740 411 8[−4]	−3.735 461 6[−4]	−3.843 386 5[−4]	−3.836 052 3[−4]
	(1,0)	−3.732 027 3[−4]	−3.727 403 5[−4]	−3.777 892 0[−4]	−3.772 701 8[−4]
1.0[−5]	(0,0)	−4.646 519 3[−4]	−4.646 488 7[−4]	−4.696 276 2[−4]	−4.696 213 7[−4]
	(0,1)	−4.485 856 1[−4]	−4.481 046 6[−4]	−4.560 416 2[−4]	−4.557 920 7[−4]
	(1,0)	−4.457 224 3[−4]	−4.453 188 1[−4]	−4.496 208 2[−4]	−4.492 079 3[−4]
1.5[−5]	(0,0)	−5.295 951 7[−4]	−5.295 951 7[−4]	−5.335 913 0[−4]	−5.335 813 2[−4]
	(0,1)	−5.117 667 3[−4]	−5.112 773 7[−4]	−5.176 737 5[−4]	−5.170 909 6[−4]
	(1,0)	−5.063 155 3[−4]	−5.059 176 6[−4]	−5.096 383 5[−4]	−5.092 463 6[−4]
2.0[−5]	(0,0)	−5.866 750 7[−4]	−5.866 618 1[−4]	−5.899 381 5[−4]	−5.899 230 2[−4]
	(0,1)	−5.670 062 8[−4]	−5.664 884 0[−4]	−5.716 231 1[−4]	−5.710 318 4[−4]
	(1,0)	−5.586 946 9[−4]	−5.582 546 6[−4]	−5.615 336 3[−4]	−5.610 970 6[−4]
	(0,2)	−5.481 781 0[−4]	−5.463 149 9[−4]	−5.542 867 5[−4]	−5.521 406 6[−4]

mates of the energies of the circular states are in excellent agreement with quantum results, while this is less so for the excited states in the manifold.

Table II deals with the set of results corresponding to field strengths in the regions where the field ionization (i.e., imaginary parts of resonance eigenvalues) is not negligible. Nevertheless one can see that semiclassical estimates still represent a fairly good approximation for the real parts of the complex eigenvalues, especially for the circular states.

Finally, in order to test the quality of semiclassical wave functions given by Eq. (2.18), we have used them to calculate the radiative lifetimes of circular Rydberg states for a number of combinations of the field strengths for which the ionization widths are negligible. The only allowed radiative, electric-dipole transition from a circular state is to the neighboring circular state with one less quantum of angular momentum: $m\rightarrow m'$, $|m'|=|m|-1$. The lifetime τ_m of a circular state is therefore given by

$$\tau_m^{-1}=\frac{4}{3c^3}(E_m-E_{m'})^3|d_{m',m}|^2, \tag{4.1}$$

TABLE II. Comparison of the calculated quantum complex eigenenergies E (in a.u.) of circular and near-circular states corresponding to $m=-40$ with semiclassical estimates E^{SC} for various fields (in a.u.) in the region where the resonance width is important. The energies of the states with $m=+40$ are obtained by adding mB. Numbers in square brackets indicate powers of ten.

F	B	(ν_1,ν_2)	E	E^{SC}
1.0[−7]	1.0[−5]	(0,0)	−4.893 145 8[−4]−i6.133 77[−7]	−4.893 780 7[−4]
		(0,1)	−4.851 246[−4]−i4.483[−6]	−4.854 250 1[−4]
		(1,0)	−4.702 335[−4]−i1.8779[−6]	−4.698 568 6[−4]
	1.5[−5]	(0,0)	−5.472 293 6[−4][a]	−5.471 943 0[−4]
		(0,1)	−5.370 992 6[−4]−i2.521[−9]	−5.358 575 8[−4]
		(1,0)	−5.228 107 5[−4]−i6.133[−9]	−5.223 289 4[−4]
	2.0[−5]	(0,0)	−6.005 402 7[−4]	−6.005 137 2[−4]
		(0,1)	−5.862 392 4[−4]	−5.853 342 6[−4]
		(1,0)	−5.713 409 6[−4]	−5.710 493 2[−4]
		(0,2)	−5.736 462 8[−4]	−5.701 548 1[−4]
1.3[−7]	1.5[−5]	(0,0)	−5.649 978 4[−4]−i2.318 59[−6]	...[b]
		(0,1)	−5.602 928[−4]−i8.239[−6]	...
		(1,0)	−5.414 596 8[−4]−i4.093 43[−6]	...
	2.0[−5]	(0,0)	−6.120 031 5[−4]−i9.559[−11]	−6.119 236 1[−4]
		(0,1)	−6.030 613 3[−4]−i2.119 26[−7]	−6.008 193 4[−4]
		(1,0)	−5.830 829 5[−4]−i8.927[−9]	−5.824 997 0[−4]
		(0,2)	−5.972 923 1[−4]−i3.3144[−6]	−5.897 150 7[−4]

[a]When the imaginary part is missing it means that it is less than 10^{-12} a.u.

[b]Above the classical ionization threshold.

TABLE III. Comparison of the calculated exact quantum radiative lifetimes τ (in msec) of circular states corresponding to $m=\mp 40$ with semiclassical estimates τ^{SC} as a function of various field strengths (in a.u.). Numbers in square brackets indicate powers of ten.

		$m=-40$		$m=+40$	
F	B	τ	τ^{SC}	τ	τ^{SC}
0	0	10.55	10.71	10.55	10.71
	0.5[−5]	15.88	16.08	6.115	6.190
	1.0[−5]	20.14	20.31	3.561	3.590
	1.5[−5]	22.95	23.08	2.233	2.245
	2.0[−5]	24.70	24.79	1.507	1.512
0.3[−7]	0	11.07	11.26	11.07	11.26
	0.5[−5]	16.66	16.88	6.307	6.392
	1.0[−5]	20.90	21.09	3.620	3.652
	1.5[−5]	23.58	23.71	2.253	2.266
	2.0[−5]	25.19	25.29	1.515	1.521
0.5[−7]	0	12.36	12.61	12.36	12.61
	0.5[−5]	18.47	18.77	6.738	6.847
	1.0[−5]	22.50	22.72	3.739	3.777
	1.5[−5]	24.82	24.98	2.292	2.306
	2.0[−5]	26.15	26.26	1.530	1.537
0.8[−7]	1.0[−5]	29.00	29.38	4.180	4.240
	1.5[−5]	28.87	29.10	2.408	2.427
	2.0[−5]	28.97	29.11	1.572	1.580
1.0[−7]	1.5[−5]	35.15	35.49	2.568	2.595
	2.0[−5]	32.48	32.67	1.619	1.629

with the dipole matrix element ($m'=m\pm 1$):

$$d_{m',m}=\mp 2^{-1/2}\langle \psi_{m'}(\rho,z,\varphi)|\rho e^{\pm i\varphi}|\psi_m(\rho,z,\varphi)\rangle, \tag{4.2}$$

where E_m and $\psi_m(\rho,z,\varphi)$ are the energy and the eigenfunction of the circular state. Table III shows the comparison between semiclassical and quantum results. An excellent agreement is found indicating that for these field strengths the simple product of two Gaussians (2.18) is a very good approximation to exact eigenfunctions.

V. CONCLUDING REMARKS

Circular and nearby states can be successfully described by the semiclassical theory presented in Sec. II. The condition is that the field strengths are such that the system is not close to or on the right of the classical ionization threshold curve shown in Fig. 1. The semiclassical approximation is excellent both for the eigenvalues and wave functions of the circular Rydberg states, but it subsequently becomes less accurate for nearby states in the same m manifold.

In the region close to and beyond the classical ionization threshold, fully quantum calculations based on the complex-coordinate method, discrete variable representation, and the complex Lanczos recursion method provide exact eigenvalues for the resonances emerging from the circular and nearby quasibound states. In general, the magnetic field has a stabilizing effect, reducing the electron field-ionization probability, but often characteristic oscillations of the widths can appear. For fixed nonzero values of the magnetic field strength, calculations have also shown oscillations of the widths as a function of electric field strength.

ACKNOWLEDGMENTS

T.P.G. is grateful for the hospitality shown by the Laboratoire de Dynamique des Ions, Atomes et Molécules, Université Pierre et Marie Curie where part of this work has been done. T.P.G. acknowledges support of this work by the Ministry of Science and Technology of the Republic of Serbia.

[1] R. G. Hulet, E. S. Hilfer, and D. Kleppner, Phys. Rev. Lett. **55**, 2137 (1985).
[2] E. de Prunelé, Phys. Rev. A **31**, 3593 (1985).
[3] S. B. Hansen, T. Ehrenreich, E. Horsdal-Pedersen, K. B. McAdam, and L. J. Dubé, Phys. Rev. Lett. **71**, 1522 (1993).
[4] M. F. Lundsgaard, Z. Chen, C. D. Lin, and N. Toshima, Phys. Rev. A **51**, 1347 (1995).
[5] R. G. Hulet and D. Kleppner, Phys. Rev. Lett. **51**, 1430 (1983).
[6] D. Richards, J. Phys. B **17**, 1221 (1984).
[7] W. A. Molander, C. R. Stroud, Jr., and T. F. Yeazell, J. Phys. B **19**, L461 (1986).
[8] D. Delande and J. C. Gay, Europhys. Lett. **5**, 303 (1988).
[9] J. Hare, M. Gross, and P. Goy, Phys. Rev. Lett. **61**, 1938 (1988).
[10] P. Nussenzveig, F. Bernadot, M. Brune, J. Hare, J. M. Raimond, S. Haroche, and W. Gawlik, Phys. Rev. A **48**, 3991 (1993).
[11] L. Chen, M. Cheret, F. Roussel, and G. Spiess, J. Phys. B **26**, L437 (1993).
[12] C. H. Cheng, C. Y. Lee, and T. F. Gallagher, Phys. Rev. Lett. **73**, 3078 (1994).
[13] G. Wunner, M. Kost, and H. Ruder, Phys. Rev. A **33**, 1444 (1986).
[14] T. C. Germann, J. Phys. B **28**, L531 (1995).
[15] T. P. Grozdanov, L. Andric, C. Manescu, and R. McCarroll, Phys. Rev. A **56**, 1865 (1997).
[16] C. H. Bender, L. D. Mlodinow, and N. Papanicolaou, Phys. Rev. A **25**, 1305 (1982).
[17] M. C. Gutzwiller, *Chaos in Classical and Quantum Mechanics* (Springer, New York, 1990).
[18] R. G. Newton, *Scattering Theory of Waves and Particles* (McGraw-Hill, New York, 1966).
[19] W. P. Reinhardt, Annu. Rev. Phys. Chem. **33**, 223 (1982).
[20] Y. K. Ho, Phys. Rep. **99**, 1 (1983).
[21] I. W. Herbst, Commun. Math. Phys. **64**, 279 (1979).
[22] J. C. Light, I. P. Hamilton, and J. V. Lill, J. Chem. Phys. **82**, 1400 (1985).
[23] D. Baye and M. Vincke, J. Phys. B **24**, 3551 (1991).
[24] K. M. Milfeld and N. Moiseyev, Chem. Phys. Lett. **130**, 145 (1986).
[25] I. Seipp, K. T. Taylor, and W. Schweizer, J. Phys. B **29**, 1 (1996).